

Assessing electromagnetic field exposure levels in multi-active reconfigurable intelligent surface assisted 5G network

Mohammed Ahmed Salem¹, Heng Siong Lim¹, Ming Yam Chua², Khaled Abdulaziz Alaghbari³,
Charilaos Zarakovitis⁴, Su Fong Chien⁵

¹Faculty of Engineering and Technology, Multimedia University, Bukit Beruang, Malaysia

²School of Electrical Engineering and Artificial Intelligence, Xiamen University Malaysia, Sepang, Malaysia

³Faculty of Electrical Engineering, Universiti Teknologi Malaysia, Johor Bahru, Malaysia

⁴ICT Department, AxonLogic IKE, Athens, Greece

⁵MIMOS Berhad, Kuala Lumpur, Malaysia

Article Info

Article history:

Received Nov 20, 2023

Revised Mar 19, 2024

Accepted Apr 2, 2024

Keywords:

5G mobile networks

Electromagnetic field exposure

machine learning

Millimeter wave

Power density

Reconfigurable intelligent surface

ABSTRACT

As 5G mobile networks continue to proliferate in dense urban environments, it becomes increasingly important to understand and mitigate excessive electromagnetic field (EMF) exposure. This study investigates how the downlink EMF exposure levels of 5G millimeter wave (mm-wave) mobile networks are influenced by the integration of multi-active reconfigurable intelligent surfaces (RISs), using a ray-tracing approach. Our research employs a comprehensive two-step methodology: Firstly, we introduce a new RIS-assisted 5G mm-wave network planning technique. This technique leverages a machine learning (ML) approach for the classification of multi-RIS clusters. The primary goal is to optimize coverage while minimizing the number of required RIS deployments. This is achieved by strategically placing RISs based on the ML classification, ultimately aiming to enhance network efficiency. Secondly, we conducted a thorough comparative analysis, evaluating the impact of both passive and active RISs on EMF exposure level throughout a dense urban environment. Passive RIS and active RIS differ in their adaptability to changing network conditions. The result shows that the influence of multi-active RISs on EMF exposure is significant (about 7.5 times higher) compared to passive RISs.

This is an open access article under the [CC BY-SA](https://creativecommons.org/licenses/by-sa/4.0/) license.



Corresponding Author:

Heng Siong Lim

Faculty of Engineering and Technology, Multimedia University

75450, Bukit Beruang, Malaysia

Email: hslim@mmu.edu.my

1. INTRODUCTION

To support the increased demands for improved quality-of-service (QoS) and enhanced data throughput as specified in the standards of 5G and beyond, several novel technologies will be integrated into the upgraded networks. These enhancements include the adoption of beamforming antenna arrays, the utilization of millimeter wave (mm-wave) technology, the deployment of denser network infrastructures, the implementation of large-scale distributed antenna systems with reconfigurable capability [1], [2], and the extensive use of carrier aggregation. However, it is crucial to acknowledge that these innovations raise concerns about potential health risks, as they are anticipated to result in heightened levels of human exposure to electromagnetic field (EMF) radiation. For instance, high-gain mm-wave beamforming antenna arrays can generate narrow, concentrated electromagnetic beams to facilitate signal transmission [3]–[5]. High-intensity EMF exposures may lead to an increase in the absorption of EM energy by the human body and excessive

local tissue temperature [6]. Additionally, network densification will progressively shrink the size of network cells, allowing for the deployment of more base stations (BSs) in closer proximity to users, thereby enhancing connection quality. Consequently, due to their proximity to one or more BSs, mobile users may experience increased exposure to EMF radiation [7].

Mm-wave transmission is well known to be highly sensitive to obstacles such as buildings and terrain irregularities. Therefore, in dense urban environments, the coverage of a gNodeB (gNB) utilizing mm-wave bands relies heavily on the quality of the link, including both line-of-sight (LoS) and non-LoS (NLoS) connections, between the gNB and the spatially distributed users. As a result, network design solutions associated with traditional sub-6 GHz networks are not optimized for networks operating at mm-wave frequencies. Several studies have tackled this issue by deploying multiple gNBs to minimize outage areas. However, while this approach meets the minimum required QoS, it comes with a significant increase in deployment costs and power consumption. The intricate nature of mm-wave propagation also poses a significant challenge in accurately evaluating EMF exposure levels within mobile networks operating at mm-wave frequencies. Ray-tracing simulations offer a promising solution to this challenge, providing detailed insights into signal propagation characteristics and interactions with surrounding obstacles. Chiaraviglio *et al.* [8] conducted an analysis of EMF levels in real-world pre-5G scenarios through the use of ray tracing. It is important to note that this analysis was limited to a base station with frequencies lower than 3 GHz and standard fixed-beam antenna. Chiaraviglio *et al.* [9] investigated the EMF effects of 5G base stations employing the pencil beamforming technique, specifically in terms of the power density (PD) metric. However, it is worth mentioning that the proposed EMF assessment procedure is limited to localization based beamforming and depends on the standard 3GPP propagation model [10]. Noé and Gaudaire [11] delves into the investigation of downlink EMF exposure generated by 5G beamforming antennas using ray tracing. Furthermore, the authors specifically compared the impact of various beamforming techniques on the level of EMF exposure in urban environments.

This section examines previous works relevant to network optimization and EMF exposure evaluation of reconfigurable intelligent surface (RIS)-assisted mm-wave mobile network. Recently, researchers have turned their attention to deploying RISs to optimize mm-wave signal coverage in outage areas. Integrating RISs can improve the coverage performance of mm-wave networks, particularly in NLoS scenarios, offering a cost-effective solution. Consequently, from an economic perspective, deploying RISs alongside gNBs could be a prudent strategy for significantly expanding coverage in densely populated urban environments. However, most recent works on RIS utilization in 5G network design have focused on meeting spectral efficiency (SE) or energy efficiency (EE) requirements, overlooking the EMF exposure constraint.

In the literature, few studies have investigated the EMF exposure for 5G networks assisted by RIS. These studies are summarized in Table 1. However, they have predominantly focused on the use of passive RISs.

Table 1. Related works on RIS-assisted gNB deployment and EMF exposure level

Ref.	Objective	Type of RIS	Frequency band	Channel Model	EMF metric
[12]	Optimize energy efficiency subject to EMF constraints	Passive	mm-wave	RP-PLM	SAR
[13]	Optimize exposure index subject to a minimum QoS requirement.	Passive	mm-wave	3GPP	EI
[14]	Enhance spectral efficiency while adhering to EMF constraint.	Passive	mm-wave	MPCM	P_R
[15], [16]	Optimize beamforming while adhering to EMF constraints.	Passive	mm-wave	MPCM	P_R

Notations: Specific absorption rate (SAR), exposure index (EI), radio propagation path loss model (RP-PLM), and multipath propagation channel model (MPCM).

Based on [12], the authors conclude that the use of passive RIS does not increase the amount of EMF radiation. However, the influence of active RIS on EMF exposure levels is not considered. Zhang *et al.* [17] compared the performance of an active RIS and a passive RIS based on the signal-to-noise ratio (SNR) and concluded that the SNR achieved by the active RIS was about 40 dB higher than the that achieved by the passive RIS. However, the study did not assess the impacts in terms of EMF exposure levels. These research gaps motivate us to investigate the effects of multi-active RISs in terms of EMF exposure when compared with multi-passive RISs within the same environmental scenarios. Addressing these identified gaps, this work presents the following original contributions:

- A new EMF evaluation framework for multi-RIS assisted mm-wave network: building upon our previous work [18], we extend the ray-tracing-based EMF evaluation framework by incorporating a machine learning-based multi-RIS clustering approach.

- New results on downlink EMF exposure levels of multi-active RIS assisted mm-wave network: Unlike [12], our spatial EMF distribution and user density analysis conclude that the influence of multi-active RISs on EMF exposure is significant compared to passive RISs.

The outline of this paper is organized as follows: section 2 introduces the system model and the proposed extended framework. Section 3 focuses on optimizing RIS placement, clustering, and performance comparison. In section 4, the results and discussions regarding the investigation of the impact of both passive and active RISs on EMF exposure levels in a dense urban environment are presented. Finally, section 5 summarizes the conclusions drawn in this paper.

2. SYSTEM MODEL AND PROPOSED FRAMEWORK

The proposed framework for evaluating downlink EMF exposure levels in multi-active RIS assisted mm-wave networks consists of five modules: (a) system modelling and 3D map configuration, (b) Ray-tracing simulation, (c) RISs placement, (d) ML-based clustering, and (e) post-processing. The details of the RIS placement, ML-based clustering, and post-processing modules are provided in section 3. The RIS placement and ML-based clustering modules are the core components, responsible for computing the optimal locations of the RISs and determining the minimum number of RISs required to serve the UEs. This framework serves as a comprehensive guide to addressing the primary research question: What are the impacts of using multi-active RISs in 5G networks assisted by MIMO and beamforming technique on EMF exposure levels? Figure 1 shows the flowchart of the proposed EMF evaluation framework based on ray-tracing.

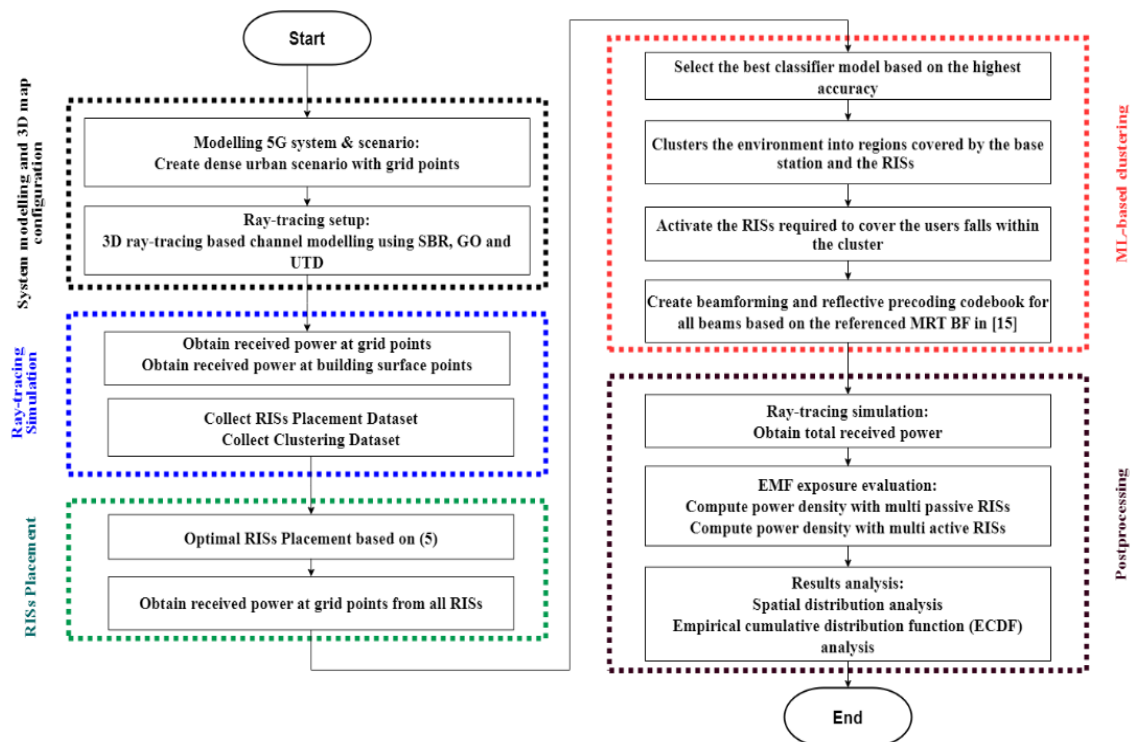


Figure 1. Flowchart of the proposed EMF evaluation framework

A 3D map is needed for ray-tracing simulation, where the EM properties of the materials such as building, and vegetation are defined according to the recommendation from previous literature. In this work, we focus on a 5G mm-wave mobile network incorporating a downlink multiple-input multiple-output (MIMO) system assisted by multi-active RISs. The system comprises of a base station (BS) with an $M \times M$ antenna array and R RISs equipped with an $N \times N$ array of reflective elements (REs) each. The base station serves K single-antenna user equipment (UE) with the assistance of the RISs. These RISs dynamically adjust the reflection beamforming (also referred to as reflecting coefficients at the REs) to control the phase shift and power amplification of the incident signals as needed. Consequently, the UE receives the signal through

two links: the RIS-aided link (BS-RIS-UE) and the direct link (BS-UE). UEs receiving signals via the direct link are considered within the base station's coverage area (base station cluster).

Ray tracing is employed to calculate the channel state information (CSI) at the transmitter by simulating the interactions of the propagation channel with the transmitted signal. To ensure the accuracy and reproducibility of our results, we utilize a commercial software package called Wireless InSite [19]. In the simulation, a 3D ray-tracing approach is employed, which integrates various techniques, including geometric optics (GO), the uniform theory of diffraction (UTD) method, and the shooting and bouncing rays (SBR) method [20], [21]. This combination enables a comprehensive modelling of electromagnetic wave behavior in complex environments. The ray paths are initiated from the source point, representing the transmitted signal, and traced as they propagate through the environment. Upon interaction with building walls and objects, the rays can undergo specular reflection. Subsequently, these reflected rays are traced, considering multiple reflections until they either reach the boundary of the study area or the maximum allowable number of reflections. The UTD and GO are then used to determine the received power at grid points and building surface points. In study [18], a detailed discussion is provided on obtaining the 5G MIMO channel coefficients and received power using 3D ray tracing. The data from grid points and building surfaces are collected for subsequent modules (RIS placement and ML-based clustering).

3. OPTIMIZATION OF RIS PLACEMENT AND CLUSTERING

The service area, defined as the outdoor areas excluding the area occupied by buildings that is served by a base station, must first be maximized using the minimum number of RISs selected from a set of possible locations. The receiver's location is considered covered if the received power at that point equals or exceeds the minimum allowable received power threshold, (or denoted as receiver sensitivity (P_{Rmin})). Conversely, if the total received power falls below P_{Rmin} , the corresponding point is classified as experiencing an outage. The value of P_{Rmin} can be derived from the mm-wave link budget analysis of 5G new radio (NR) systems [22], [23]. For example, P_{Rmin} can be expressed as follows (assuming the minimum required SNR is 0 dB):

$$P_{Rmin} = N_T + N_F + 10 \log_{10}(BW), \quad (1)$$

Considering thermal noise of $N_T = -174$ dBm/Hz, noise figure of $N_F = 10$ dB, and bandwidth of $BW = 100$ MHz, the minimum allowable received power threshold is -84 dBm. Based on this threshold, the grid points are split into two sets, namely the set of the covered area (S_{CA}) and the set of the outage area (S_{OA}). For downlink transmission, the received power can be expressed as [19].

$$P_{Rk} = |h_k^H w_k|^2 \quad (2)$$

where w_k is the beamforming weights vector for the k -th UE, $h_k = [h_k[1], \dots, h_k[N]]^T$ is the complex-valued channel coefficients vector, and $(\cdot)^H$ represents the conjugate transpose. The beamforming weights for the k -th UE is set to be proportional to the channel gains of the respective antenna elements:

$$w_k = \frac{h_k}{|h_k|} \sqrt{p_t} \quad (3)$$

where p_t is the transmitted power toward the k -th UE. In conclusion, the minimum allowable received power threshold expressed in (1) and the received power expressed in (2) are used to satisfy Constraint (b) in (5.2). We assume the RISs can only be placed on the outer surfaces of buildings and can be oriented in any direction. The set of building surface locations can be expressed as 3D coordinates [24].

$$S_{build} = \{(x_b, y_b, z_b) | \forall b \in B\} \quad (4)$$

where B is the set of all points on the outer surface of the buildings. The set of all visible points (LoS) on the buildings from the base station and from the points in S_{OA} are denoted as S_{VBS} and S_{VOA} , respectively. The datasets S_{build} , S_{VBS} , and S_{VOA} are derived from the simulation using Wireless InSite. The set of candidate locations for the RISs (S_{CRISs}) comprises the intersection points of the three datasets (S_{build} , S_{VBS} , and S_{VOA}). The locations to deploy the R RISs ($S_{RIS} = \{(x_1^*, y_1^*, z_1^*), \dots, (x_R^*, y_R^*, z_R^*)\}$) are decided by maximizing the *Enhanced Coverage*, which is defined as the ratio of $|S_{COA}|$ (the portion of the outage area that is now covered due to the utilization of RISs) to the outage area ($|S_{OA}|$). This metric quantifies the improvement in coverage achieved by deploying RISs. The placement optimization problem (POP) is defined as follows:

3.1. Placement optimization problem (POP)

The placement optimization problem is defined as follows:

$$\underset{S_{RIS}}{\text{Max Enhanced Coverage}} = \frac{|S_{COA}|}{|S_{OA}|} \times 100\% \quad (5)$$

$$\text{s. t. } \{(x_i, y_i, z_i) \in [S_{VBS} \cap S_{VOA} \cap S_{build}]\} \text{ for } i = 1, \dots, R \quad (5.1)$$

$$S_{COA} = \{k | P_{Rk} \geq P_{Rmin}, k \in S_{OA}\} \quad (5.2)$$

where $|\cdot|$ is the cardinality of a set. Constraint (5.1) ensures that the optimal location of the RIS belongs to the set of candidates RIS locations. Constraint (5.2) ensures that the receiver locations having received power exceeding the minimum allowable received power threshold are counted as under coverage. After solving the placement optimization problem, we find the optimal locations for the RISs to cover the service area. Then, each RIS is assigned to cover a specific territory on the map. The assignments can be done by using machine learning classifiers such as random forest (RF) [25], support vector machine (SVM) [26], naive bayes (NB) [27], decision tree (DT) [28], k-nearest neighbor (K-NN) [28], and deep neural network (DNN) [29]. This process clusters the environment into regions covered by the base station and the RISs. The features extracted from the grid points data are the location of the grid points (X, Y, Z) and the received power from the base station (P_{RBS}) and received power from each RIS ($P_{RRIS,i}$).

In this paper, we compare the impacts of utilizing passive and active RISs on the EMF radiation exposure level for a dense urban environment. The comparison is carried out by placing the RISs at optimized locations to cover the UEs. For a fair comparison, we constrain the total transmit power of the two scenarios to 1W (30 dBm) by setting the BS transmit power to 1W for the passive multi-RIS-aided system and $1/(R + 1)$ W, for the active multi-RIS-aided system.

4. RESULTS AND DISCUSSION

Table 2 shows the simulation parameters considered for the 5G dense urban network. For the downlink, complex-valued path gains for each sub-channel between the BS and the UEs were obtained from a realistic ray tracing simulator (Wireless InSite) to calculate the beamforming (or precoding) weights. These precoding weights are calculated using the maximum ratio transmission (MRT) beamforming technique [16] to ensure that the UEs receive the maximum power. Then, the received power for the entire study area is simulated and used to evaluate the EMF exposure level. Throughout this paper, all simulations and results are for a small cell scenario in the dense urban city of Rosslyn, Virginia, shown in Figure 2. According to Salem *et al.* [18], for a dense urban setting, the anticipated size of population in this area consists of 123 people. The locations of these UEs were randomly distributed, with 93 UEs outdoors and 30 UEs indoors within buildings. It is important to note that, in this study, the assessment of EMF exposure was focused exclusively on the outdoor UEs.

Six machine-learning-based classifiers were used for the clustering process, and their performances were evaluated based on accuracy to determine the top-performing classifier. These classifiers were trained using a dataset containing 4 features extracted from the data, with 70% of the data allocated for training, 15% for testing, and the remaining 15% for validation. The ML and DL toolbox (classifier learner) in MATLAB 2021b was utilized for this purpose. The comparison of the different classifiers revealed that the K-NN model achieved the highest accuracy at 98.2%, as indicated in Table 3.

Figure 3 illustrates the coverage analysis, optimized RISs placement and clustering. The area covered by the BS (without utilizing RISs) is shown in Figure 3(a), comprising 52.4% of the total area. Conversely, 47.6% of the service area was left uncovered. Figure 3(b) illustrates the clusters assigned to each RIS node, with eight RISs utilized to enhance coverage. The proposed RIS clustering technique facilitates the organization of the transmission flow for the RIS-assisted link (BS-RIS-UE). Consequently, the base station can intelligently direct its beams towards the appropriate RIS to ensure coverage of the UEs within the outage areas. The proposed clustering technique streamlines the deployment and activation of the RISs for urban UE coverage. In Figure 3(c), the tangible outcome is apparent: only three (RIS 1, RIS 7, and RIS 8) out of eight available RISs are required to be activated to seamlessly serve 93 randomly distributed UEs. This strategic allocation underscores the practical efficiency of our approach, permitting deactivation of some of the deployed RISs without compromising comprehensive coverage. Based on Figure 3(c), we observed that one UE was not covered because it was located within the building. In Figure 3(d), the optimal location of each RIS is presented with the percentage of the enhanced coverage.

Figure 4 demonstrates the comparison between multi-active RISs and multi-passive RISs based on the EMF exposure level within the entire service area. Figure 4(a) shows the plot of the average and peak values of the total power density (PD) versus distance from the BS for both scenarios considered. Additionally, Figure 4(a) displays the maximum limit set by International Commission on Non-Ionizing Radiation Protection (ICNIRP). The PD was observed to be mainly dependent on three factors: the distance from the base station, the concentration of the UEs in a specific area, and the type of RISs used.

Parameters	Description
5G System & Scenario	
BS antenna	8×8 array per data stream
Frequency	28 GHz
BS height	10 m
BS Tx power with pRIS	30 dBm
BS Tx power with aRIS	23.9794 dBm
UE antenna	Single halfwave dipole
UE height	2 m
RIS elements	10×10
ARISs power	23.9794 dBm
Ray-Tracing Parameters	
Propagation model	Full 3D (X3D)
Ray tracing technique	SBR
Ray spacing	0.15
Number of paths	25
Number of reflections	6
Coverage Analysis	
Minimum allowable received power threshold (P_{Rmin})	-84 dBm
Percentage of S_{CA}	52.3979%
Percentage of S_{OA}	47.6021%
EM Properties of Materials	
Material	ϵ_r $\sigma[S/m]$
Vegetation-Branch	20 0.39
Vegetation-Leaf	26 0.39
Buildings (Concrete)	5.31 0.8967

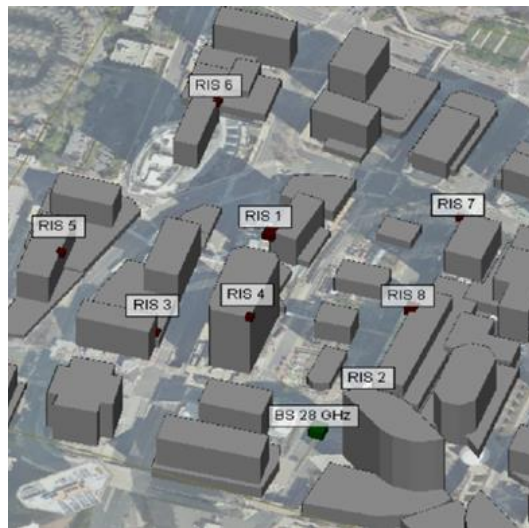


Figure 2. Locations of the base station and RISs in a dense urban environment

Table 3. Comparison of different classifiers

Classifier	Accuracy (%)
Decision tree	96.5
SVM	97.3
KNN (K=7)	98.2 (Selected)
Naive Bayes	86.9
Random forest	97.4
Deep neural network	96.1

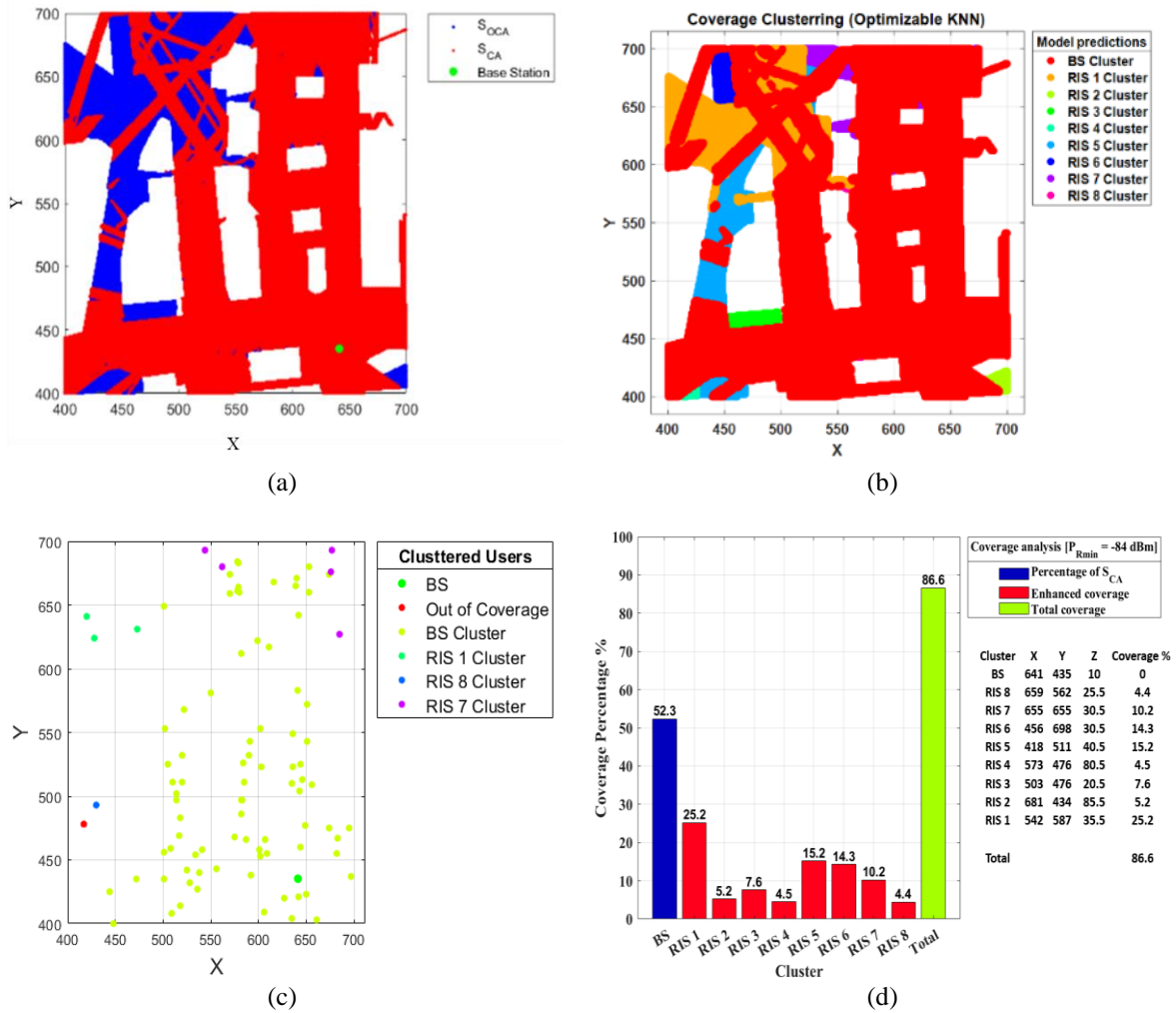


Figure 3. Coverage, placement and clustering analysis (a) base station location, covered area, and outage area, (b) RIS clusters, (c) UE's coverage, and (d) RISs optimal locations and percentage of enhanced coverage

In general, the PD decreased with increasing distance. However, there were instances where the total PD was higher at certain spots far from the base station compared to those closer to it. This phenomenon can be attributed to the higher density of UEs operating near each other in those areas. We observed that the maximum EMF level without using RISs was similar to the EMF level when using passive RISs. The main reason for this similarity is that the passive elements of the RIS did not receive amplified power. Consequently, the signal with the same incident power was reflected (assuming ideal passive reflection). A similar observation was also reported in [12]. However, the utilization of active RISs led to elevated EMF levels. According to Figure 4(a), the maximum PD observed due to the use of passive RISs is 24.92 dBm/m² (62% of ICNIRP's limit), whereas the maximum PD observed due to the use of active RISs is 33.65 dBm/m² (84% of ICNIRP's limit), which is about 7.5 times higher than when using passive RISs. Unlike [12], our analysis demonstrates that the impact of multi-active RISs on EMF exposure is significant, being 7.5 times higher compared to passive RISs. Figure 4(b) depicts the empirical cumulative distribution function (ECDF) of the PD levels in the studied area, which included 93 active outdoor UEs. According to Figure 4(b), considering multi-active RISs, there is a 10% probability that the PD may exceed 30 dBm/m², equivalent to 75% of the ICNIRP's limit. Figures 4(c) and 4(d) depict the spatial distribution of total PD attributed to passive and active RISs in a dense urban environment. It is evident that the EMF level in the study area increased significantly when each UE located in outage areas was actively served by the active RISs. This scenario demonstrates that almost all areas that previously had low levels of EMF exposure (when passive RISs were activated) were now experiencing high EMF exposure.

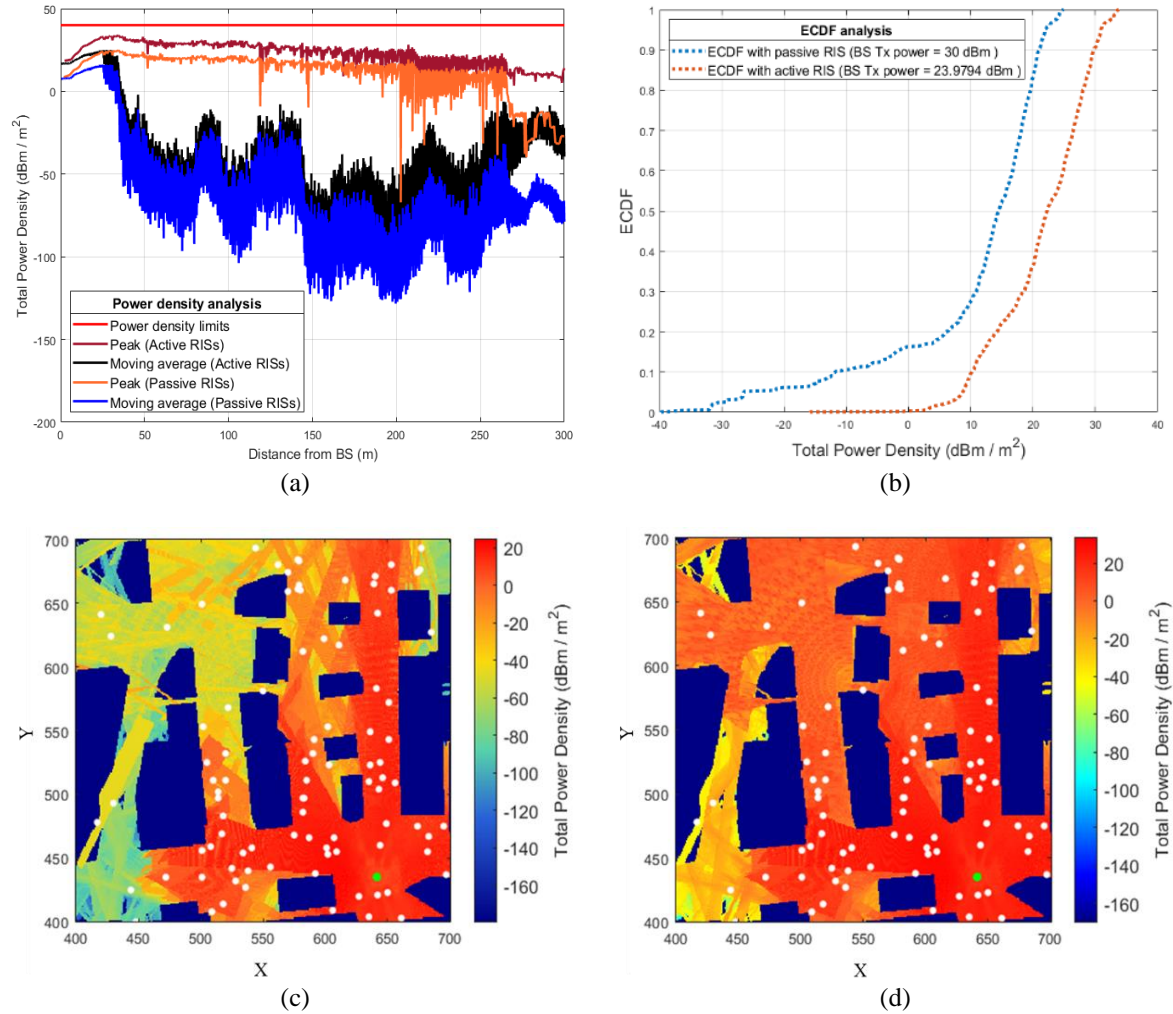


Figure 4. EMF evaluation analysis (a) downlink PD, (b) ECDF of PD, (c) spatial distribution of PD (multi-passive RIS), and (d) spatial distribution of PD (multi-active RIS)

5. CONCLUSION

This research investigates the EMF exposure intensity, measured by the PD metric, of a multi-RISs-assisted 5G mm-wave network utilizing MIMO beamforming in downlink transmissions. The findings indicate that the PD metric remained below the thresholds established by ICNIRP. However, the use of multi-active RISs resulted in a significant increase in exposure levels. It is noteworthy that in environments with higher UE density, the exposure to EMF could potentially increase even further. For future work, we plan to optimize the energy efficiency (EE) of active-RIS-assisted 5G mm-wave networks while considering both EMF exposure and power constraints. One potential avenue involves developing a joint optimization algorithm that addresses both EMF exposure and power constraints. Overall, devising EMF-aware algorithms for multi-active RIS-assisted 5G networks can offer valuable insights into the design and optimization of such networks, balancing energy efficiency with safe EMF exposure levels.

ACKNOWLEDGEMENTS

This research is supported by the Fundamental Research Grant Scheme of the Malaysian Ministry of Higher Education under Grant no. FRGS/1/2020/ICT09/MMU/02/1.




REFERENCES

- [1] A. K. Abd and J. M. Rasool, "Low-profile frequency-reconfigurable antenna for 5G applications," *TELKOMNIKA (Telecommunication Computing Electronics and Control)*, vol. 21, no. 3, pp. 486–495, Jun. 2023, doi: 10.12928/telkomnika.v21i3.24028.




- [2] S. A. Refaat, H. A. Mohamed, A. M. Abdelhady, and A. S. Mohra, "A 28/38 GHz tuned reconfigurable antenna for 5G mobile communications," *Indonesian Journal of Electrical Engineering and Computer Science (IJECS)*, vol. 31, no. 1, pp. 248–258, Jul. 2023, doi: 10.11591/ijeecs.v31.i1.pp248-258.
- [3] B. Thors, A. Furuskar, D. Colombi, and C. Tornevik, "Time-averaged realistic maximum power levels for the assessment of radio frequency exposure for 5G radio base stations using massive MIMO," *IEEE Access*, vol. 5, pp. 19711–19719, 2017, doi: 10.1109/ACCESS.2017.2753459.
- [4] D. Colombi, B. Thors, C. Tornevik, and Q. Balzano, "RF energy absorption by biological tissues in close proximity to millimeter-wave 5G wireless equipment," *IEEE Access*, vol. 6, pp. 4974–4981, 2018, doi: 10.1109/ACCESS.2018.2790038.
- [5] D. Colombi, B. Thors, and C. Tornevik, "Implications of EMF exposure limits on output power levels for 5G devices above 6 GHz," *IEEE Antennas and Wireless Propagation Letters*, vol. 14, pp. 1247–1249, 2015, doi: 10.1109/LAWP.2015.2400331.
- [6] R. Dilli, "Implications of mmWave radiation on human health : state of the art threshold levels," *IEEE Access*, vol. 9, pp. 13009–13021, 2021, doi: 10.1109/ACCESS.2021.3052387.
- [7] M. Agiwal, A. Roy, and N. Saxena, "Next generation 5G wireless networks: a comprehensive survey," *IEEE Communications Surveys & Tutorials*, vol. 18, no. 3, pp. 1617–1655, 2016, doi: 10.1109/COMST.2016.2532458.
- [8] L. Chiaraviglio, A. S. Cacciapuoti, G. D. I. Martino, M. Fiore, M. Montesano, and D. Trucchi, "Planning 5G networks under EMF constraints : state of the art and vision," *IEEE Access*, vol. 6, pp. 51021–51037, 2018, doi: 10.1109/ACCESS.2018.2868347.
- [9] L. Chiaraviglio, S. Rossetti, S. Saida, S. Bartoletti, and N. Blefari-Melazzi, "Pencil beamforming increases human exposure to electromagnetic fields: true or false?," *IEEE Access*, vol. 9, pp. 25158–25171, 2021, doi: 10.1109/ACCESS.2021.3057237.
- [10] 3GPP, "Study on channel model for frequencies from 0.5 to 100 GHz," *3GPP TR 38.901 V15.1.0*, 2019.
- [11] N. Noé and F. Gaudaire, "Numerical modeling of downlink electromagnetic wave exposure generated by 5G beamforming antennas," *Comptes Rendus Physique*, vol. 22, no. S1, pp. 15–24, 2021, doi: 10.5802/crphys.61.
- [12] A. Zappone and M. Di Renzo, "Energy efficiency optimization of reconfigurable intelligent surfaces with electromagnetic field exposure constraints," *IEEE Signal Processing Letters*, pp. 1–5, 2022, doi: 10.1109/lsp.2022.3181532.
- [13] H. Ibraiwish, A. Elzanaty, Y. H. Al-Badarnah, and M. S. Alouini, "EMF-aware cellular networks in RIS-assisted environments," *IEEE Communications Letters*, vol. 26, no. 1, pp. 123–127, 2022, doi: 10.1109/LCOMM.2021.3120688.
- [14] N. Awarkeh, D. T. Phan-Huy, and R. Visoz, "Electro-magnetic field (EMF) aware beamforming assisted by reconfigurable intelligent surfaces," *IEEE Workshop on Signal Processing Advances in Wireless Communications, SPAWC*, vol. 2021-Sept, pp. 541–545, 2021, doi: 10.1109/SPAWC51858.2021.9593226.
- [15] N. Awarkeh and M. Di Renzo, "A novel RIS-Aided EMF exposure aware approach using an angularly equalized virtual propagation channel," *Joint European Conference on Networks and Communications & 6G Summit (EuCNC/6G Summit)*, 2022, doi: 10.1109/EuCNC/6GSummit54941.2022.9815608.
- [16] N. Awarkeh, D. T. Phan-Huy, R. Visoz, and M. Di Renzo, "A novel RIS-Aided EMF-aware beamforming using directional spreading, truncation and boosting," *2022 Joint European Conference on Networks and Communications and 6G Summit, EuCNC/6G Summit 2022*, pp. 7–12, 2022, doi: 10.1109/EuCNC/6GSummit54941.2022.9815800.
- [17] Z. Zhang *et al.*, "Active RIS vs. passive RIS: which will prevail in 6G?," *IEEE Transactions on Communications*, vol. 71, no. 3, pp. 1707–1725, Mar. 2023, doi: 10.1109/TCOMM.2022.3231893.
- [18] M. A. Salem *et al.*, "Investigation of EMF exposure level for uplink and downlink of 5G network using ray tracing approach," *International Journal of Technology*, vol. 13, no. 6, 2022, doi: 10.14716/ijtech.v13i6.5928.
- [19] I. Remcom, "Wireless InSite Reference Manual," *Version 2.8.1, Remcom, Inc. Manual*, 2016.
- [20] J. Schuster and R. Luebbers, "Comparison of site-specific radio propagation path loss predictions to measurements in an urban area," in *IEEE Antennas and Propagation Society International Symposium. 1996 Digest*, 1996, vol. 2, pp. 1210–1213, doi: 10.1109/APS.1996.549814.
- [21] J. Schuster and R. Luebbers, "Hybrid SBR/GTD radio propagation model for site-specific predictions in an urban environment," *12th Annual Rev. of Progress in Applied Computational Electromagnetics*, vol. 1, pp. 84–92, 1996.
- [22] Telecom trainer team, "5G mmWave 28 GHz band link budget analysis online tool," *Techplayon*, 2020.
- [23] A. Roessler, "Pre-5G and 5G: Will the mmwave link work?," *Microwave Journal*, vol. 60, no. 12, pp. 56–72, 2017.
- [24] C. K. Anjinappa, F. Erden, and I. Guvenc, "Base station and passive reflectors placement for urban mmwave networks," *IEEE Transactions on Vehicular Technology*, vol. 70, no. 4, pp. 3525–3539, 2021, doi: 10.1109/TVT.2021.3065221.
- [25] L. Briman, "Random Forests," *Machine learning*, pp. 542–545, 2001, doi: 10.1109/ICCECE51280.2021.9342376.
- [26] C. Cortes and V. Vapnik, "Support-vector networks," *Machine Learning*, vol. 20, no. 3, pp. 273–297, Sep. 1995, doi: 10.1007/BF00994018.
- [27] H. Zhang, "The optimality of Naive Bayes," *Proceedings of the Seventeenth International Florida Artificial Intelligence Research Society Conference, FLAIRS 2004*, vol. 2, pp. 562–567, 2004.
- [28] J. R. Quinlan, "Induction of decision trees," *Machine Learning*, vol. 1, no. 1, pp. 81–106, 1986, doi: 10.1007/bf00116251.
- [29] Y. LeCun, Y. Bengio, and G. Hinton, "Deep learning," *Nature*, vol. 521, no. 7553, pp. 436–444, May 2015, doi: 10.1038/nature14539.

BIOGRAPHIES OF AUTHORS






Mohammed Ahmed Salem    received the B.S. degree in mechatronics engineering from Universiti Teknikal Malaysia Melaka (UTeM), Malaysia, in 2017. He is currently pursuing the Ph.D. degree in telecommunication engineering at Multimedia University (MMU), Malaysia. His research interests include wireless physical layer security, cooperative relay networks, non-orthogonal multi access network, RIS-assisted 5G resource allocations, and EMF evaluation. He can be contacted at email: mohammedmmu94@gmail.com.






Heng Siong Lim    (Senior Member, IEEE) received the B.Eng. degree (Hons.) in electrical engineering from Universiti Teknologi Malaysia, Malaysia, in 1999, and the M.Eng.Sc. and Ph.D. degrees in wireless communications from Multimedia University, Malaysia, in 2002 and 2008, respectively. He is currently a professor with the Faculty of Engineering and Technology, Multimedia University. His research interests include the areas of signal processing for wireless communications and advanced digital communication receiver's design. He can be contacted at email: hslim@mmu.edu.my.






Ming Yam Chua    (Member, IEEE) was born in Malacca, Malaysia, in 1980. He received the B.Eng. degree (Hons.) in electronics, and the M.Eng.Sc. and Ph.D. degrees in engineering, with a focus in radar system design and radar waveform synthesis techniques, from Multimedia University, Selangor, Malaysia, in 2003, 2007, and 2016, respectively. He was with Multimedia University as a researcher from 2003 to 2009, a lecturer from 2009 to 2012, and a senior lecturer from 2012 to 2016. He is currently an assistant professor with the Center for Environmental Remote Sensing, Chiba University, Chiba, Japan, for his two years of the postdoctoral research fellowship. His research interests include synthetic aperture radar system development, field-programmable gate array applications for the radar system, and embedded system design. He can be contacted at email: mychua1221@gmail.com.






Khaled Abdulaziz Alaghbari    received the B.Eng. degree (Hons.) in electronics engineering majoring in telecommunication and the M.Eng.Sc. and Ph.D. degrees from Multimedia University (MMU), Malacca, Malaysia, in 2011, 2014, and 2020, respectively. He was a postdoctoral researcher with the Institute of IR 4.0, National University of Malaysia (UKM), from 2021 to 2022. He is currently a postdoctoral research fellow with the center for sustainable communications and IoT, MMU. His research interests include signal processing, communication systems, and artificial intelligence (AI). He can be contacted at email: abdulazizabdullah.k@utm.my.



Charilaos Zarakovitis    received the BSc, two MScs, an MPhil, and PhD degrees in electronic engineering. He has academic experience gained at NCSR GR, TEI Piraeus GR, ULancaster UK, USurrey UK, UBrunel UK, and DIT IE as well as industrial experience gained at Motorola UK and Intracom GR, where he offered services in scientific research and development. His research interests include the design and decision-making in green communications systems, cyber physical systems, cognitive radios, visible light communications systems, vehicular networks, neural networks, in the sense of developing novel and optimized solutions based on distributed computing, machine learning, evolutionary bio-inspired computation, network virtualization, system and control theory, game theory, probability theory, and quantum theory and convex analysis. His publications in these fields have attracted 500+ citations, with the H-index of 8. He can be contacted at email: c.zarakovitis@iit.demokritos.gr.



Su Fong Chien    (SM'08) was born in Melaka, Malaysia, in 1970. He received the B.Sc. and M.Sc. degrees from the University of Malaya, Malaysia, in 1995 and 1998, respectively, and the Ph.D. degree from Multimedia University, Malaysia, in 2002. He is currently working as a principal researcher with Applied Mathematics Laboratory, MIMOS Berhad, Malaysia. He has been serving as a TPC member or a reviewer for ICACCI, ICP, SETCAC, ISCIT, GNDS, ad hoc networks, and CNCT. He has published several conference and refereed journal papers and holds a patent. His current research interests include green communications, bio-inspired algorithm applications, and optimization. He is one of the editors-in-chief of bio-inspired computation in telecommunications. He can be contacted at email: sufong.chien@gmail.com.